Assessment of Yb^{3+} ion pairs effect on a highly Yb-doped double-clad fibre laser

J A Vallés[1], J C Martín[1], V Berdejo[2], R. Cases[3], J M Álvarez[1], M Á Rebolledo[1]
[1]Department of Applied Physics and I3A, University of Zaragoza, Spain
[2]Department of Applied Physics, University Polytechnic School, La Almunia, Zaragoza, Spain
[3]Department of Condensed Matter and ICMA, University of Zaragoza, Spain

E-mail: juanval@unizar.es

Abstract. Using a previously validated characterization method based on the careful measurement of the characteristic parameters and fluorescence emission spectra of a highly Yb-doped double-clad fibre, the contribution of ion-pairs induced processes to the output power of a double-clad Yb-doped fibre ring laser is evaluated. This contribution is proved to be insignificant, contrarily to analysis by other authors, where the role of ion-pairs is overestimated.

1. Introduction

Recently, the development of new fibre designs and pumping configurations have allowed the increase in pump efficiency required for fibre lasers power scaling. In particular, the cladding pump scheme together with high-power multimode diode lasers as pump sources enables very high pump launch efficiency with relatively uncritical alignment tolerances [1,2]. Due to its excellent power conversion efficiency and broad gain bandwidth the Yb^{3+} ion is especially attractive for high output devices in the 1.0-1.2 μm spectral range (with output powers in the kW level) [3-6] but depending on the host material the required high dopant concentrations may increase migration-enhanced nonradiative losses, radiation trapping [7-9], Yb^{3+} ion pairs (IPs)-induced cooperative processes [10,11] or clustering effects as the photoinduced absorption in the visible range [12]. The real impact of some of these processes in the performance of Yb-doped amplifiers or lasers is still unclear.

In a previous paper we presented a characterization method for a highly Yb-doped double clad fibre and its experimental verification on measurements of a ring-cavity laser using as active medium two Yb-doped fibres with different dopant concentration and lengths [13]. There, it was concluded that, when modelling Yb-doped active devices the role of Yb^{3+} ion pairs (IPs) has sometimes been overestimated. In particular, in Ref. [14] when characterizing highly-doped double-clad fibres the concentration dependence of some parameters as, for instance, excited state lifetime or absorption/emission cross sections has been neglected, incorrectly assigning the laser performance concentration dependence to IP induced mechanisms.

In order to further clarify the impact of cooperative processes in highly Yb-doped lasers performance in this paper we present an evaluation of the effective influence of IPs in the laser output power by comparing numerical simulations to the experimental output power of a ring configuration double-clad Yb-doped fibre laser. In section 2 the Yb^{3+}-ion pairs induced processes are examined and the model used for the numerical simulations is resumed. Characterization measurements on DC Yb-doped fibres in the visible range are shown in section 3 together with the laser setup used to measure the laser output power with different dopant

concentrations, fibre lengths and laser ring output coupler rates in order to unequivocally validate the model presented in Ref. [13]. Finally, in section 4 the actual effect of IPs induced processes is analysed by incorporating their influence in the previously tested model as a function of the cooperative coefficient.

2. Theoretical model

2.1. Yb^{3+}-ion spectroscopy

Compared to other rare earth ions the energy level structure of the Yb^{3+} ion is simpler. With the ground electronic state $4f^{13}$ configuration only two level manifolds are relevant, those of the $^2F_{7/2}$ ground state and the $^2F_{5/2}$ excited state, which are split in 4 and 3 Stark levels, respectively. Therefore, pump or signal/laser light excited-state absorption or ion-ion energy transfer processes such as the concentration-dependent homogeneous upconversion or cross-relaxation process do not occur. Because of the large energy gap between Yb^{3+} ground and metastable multiplets non-radiative de-excitation processes such as multi-phonon relaxation are unlikely in Yb^{3+} [15]. The large overlapping between absorption and emission spectra in the Yb^{3+} ion favours the effect of strongly concentration-dependent mechanisms such as nonradiative decay due to migration through excited Yb^{3+} ions to isolated impurity traps (OH^- groups or uncontrolled rare earth ions) or radiation trapping (spontaneously emitted photons trapped by reabsorption by Yb^{3+} ions in the $^2F_{7/2}$ ground state and subsequently reemitted). Non-radiative losses and trapping of radiation have opposite effects on the $^2F_{5/2}$–level lifetime [7].

2.2. Yb^{3+}-pairs and cooperative processes.

Additional losses could be induced by clustering of Yb^{3+} ions in a heavily-doped host with limited solubility. The existence of Yb^{3+}-ion pairs (IPs) leads to cooperative processes where the two Yb^{3+} ions may emit or absorb collectively. In the first case, cooperative luminescence (CL), two interacting excited ions decay simultaneously to the ground state emitting one single photon in the visible spectral range at twice the energy of the single transition, whereas in the second the IPs may absorb in the visible [10,11,14]. Since cooperative processes rely on electrostatic interaction between ions, they have a strong dependence on inter-ionic distances and accordingly on the ion concentration.

Yb^{3+} IPs cooperative processes were already reported in the 70s [10] and have been investigated in a variety of glass [16,17], crystalline [18-20] ceramic [21] and waveguiding systems [22-24]. Even the analysis of the correlation between cooperative luminescence and photodarkening (PD) has contributed to the PD mechanism description [25]. Although IPs limit amplifier/laser performance, proposed applications for cooperative emission are 3D planar displays, intrinsic bistability for optical switching and planar lasers for optical devices in telecommunications [26]. The real influence of Yb^{3+} IPs cooperative processes in the performance of Yb-doped fibre amplifiers/lasers is still unclear. Most authors state that the influence of IP on the excited-state population dynamics is very small based on the fact that the cooperative emission is very weak compared with the NIR emission [8]. On the contrary, in Ref. [14] an experimental and theoretical investigation of the nonlinear transmission coefficient in a set of Ytterbium-doped silica fibers (YFs) with various concentrations of Yb^{3+} ions at cw 980-nm pumping concluded that YF transmission coefficient and excited-state relaxation were notably affected by the presence of Yb^{3+} - Yb^{3+} ion-pairs in the fibres.

Upconverted cooperative luminescence of three Yb^{3+} ions has been observed in the UV region under NIR excitation. The formation of Yb^{3+} clusters containing closely spaced ions was demonstrated to favour the occurrence of these multi-ion interaction processes [27]. Finally, a cooperative effect involving the simultaneous IR-pumping induced excitation of a cluster composed of several closely spaced Yb^{3+} ions has been proposed as the origin of a colour centre generation in the core glass network and the subsequent excitation energy transfer to the transitions responsible for the absorption in the visible range (PD effect) [12]. This photoinduced increase in optical loss is considered to be the critical factor for high power fibre

lasers power stability. The correlation between CL and PD dynamics has been investigated in order to gain insight into the PD mechanism [28].

2.3. Rate equations

If ytterbium ions are confined in the fibre core with a constant density, n_{Yb}, the population densities n_1 and n_2 of states $^2F_{7/2}$ and $^2F_{5/2}$, respectively, are related by the equation $n_1 + n_2 = n_{Yb}$, where dependence of n_i on the radial (r), athimutal (φ)and axial coordinates (z) is omitted for the sake of simplicity. The local Yb^{3+} ion lower and upper state population densities are governed by the rate equations:

$$\frac{dn_1}{dt} = -W_{12}n_1 + (A_{21} + W_{21})n_2 \tag{1}$$

$$\frac{dn_2}{dt} = W_{12}n_1 - (A_{21} + W_{21})n_2 - 2C_p n_2^2 \tag{2}$$

In Eq. (1)-(2) A_{21} is the spontaneous transition rate between the excited and ground states and the densities of stimulated transition rates, W_{ij}, are:

$$W_{ij}(r,\theta,z) = \int_{\nu_{p,i}}^{\nu_{p,f}} \frac{P_p(z,\nu)\psi_p(r,\theta,\nu)}{h\nu}\sigma_{ij}(\nu)d\nu + \int_{\nu_{f,i}}^{\nu_{f,f}} \frac{\left[P_f^+(z,\nu) + P_f^-(z,\nu)\right]\psi_f(r,\theta,\nu)}{h\nu}\sigma_{ij}(\nu)d\nu \tag{3}$$

In Eq. (3) $\sigma_{ij}(\nu)$ are the cross sections related to the transition between the *ith* and *jth* levels, $\psi_\beta(r,\theta,\nu)$ is the normalized mode envelope of the pump ($\beta = p$) or ASE waves ($\beta = f$) and $P_\beta(z,\nu)$ are the optical powers. The superscript "+" denotes copropagating waves whereas "–" indicates counterpropagating waves along the z axis. In our model for the normalized mode envelopes we assume:

$$\psi_p(r) = \frac{1}{\pi R_{CLAD}^2} \quad , \quad \psi_f(r) = \frac{1}{\pi R_f^2} e^{-\frac{r^2}{R_f^2}} \tag{4}$$

where R_{CLAD} is the clad radius and R_f is the signal/laser mode radius.

If IPs are present another process has to be considered: the cooperative de-excitation of a pair of Yb^{3+} ions via the spontaneous cooperative emission. The term $-2C_p n_2^2$ with a quadratic dependence on the excited state population describes the contribution of cooperative luminescence to the single ion dynamics. In practice, it causes an effective lifetime decrease and acts as an additional loss. C_p is the cooperative coefficient which depends on the interionic distance (and accordingly on the Yb^{3+} ions concentration), the glassy host, and the multipolar coupling mechanisms.

2.4. Propagation of optical powers

The equations that express the evolution of the pump, signal and ASE powers along the active waveguide are:

$$\frac{dP_p(z,\nu)}{dz} = -\left[N_{1p}\sigma_{12}(\nu) - N_{2p}\sigma_{21}(\nu) + \alpha_p\right]P_p(z,\nu) \tag{5}$$

$$\frac{dP_f^\pm(z,\nu)}{dz} = \pm 2h\nu\Delta\nu N_{2s}\sigma_{21}(\nu) \mp \left[N_{1f}\sigma_{12}(\nu) - N_{2f}\sigma_{21}(\nu) + \alpha_f\right]P_f^\pm(z,\nu) \tag{6}$$

where $N_{i\beta}$ denotes the overlapping integral between the modal distribution, $\psi_\beta(r,\varphi,\nu)$, and the population distribution of level *ith*, $n_i(r,\varphi,z)$, that is:

$$N_{i\beta}(z,\nu) = \int_A \psi_\beta(r,\varphi,\nu)\, n_i(r,\varphi,z)\, dA \tag{7}$$

and A is the area where ytterbium ions are confined.

3. Experimental

3.1. Characterization measurements.

For the experiments we had two DC Yb-doped silica fibres from CorActive™ with different Yb^{3+} concentrations: DCF-YB-6/128 (F#1) and DCF-YB-8/128P-FA (F#2). Fibres provider assures single-mode operation and photodarkening-free performance. In table I the main fibre parameters are summarized.

Table I. Parameters of the two Yb-doped fibres used in the experiments

Parameter	F#1	F#2
Core diameter (μm)	6.8	8.1
Inner-cladding diameter (μm)	129	127
Outer-cladding diameter (μm)	267	255
Effective N.A.	0.154	0.102
Absorption Yb 915 nm (dB/m)	0.7	1.7
Absorption Yb 974 nm (dB/m)	3	11
IR lifetime (ms)	0.82	1.43
Yb ion concentration ($x10^{26}$ m^{-3})	3.6	12

Under 980 nm excitation both DC Yb-doped silica fibres shown visible luminescence at $\lambda \approx 0.5$ μm. Transversal fluorescence in the visible region was detected through a 0.5 JARREL-ASH monochromator with a Hamamatsu R928 photomultiplier tube. Measurements were registered through the fibre lateral surface near the pump-input end, thus avoiding re-absorption effects. Due to the different measurement procedures the cooperative and IR luminescence powers cannot be directly compared. Cooperative luminescence of both samples is shown in Fig. 1. HWHM (half width at half maximum) is 20 nm, approximately. The peaks at 488 nm could be related to transitions between Stark levels of isolated Yb^{3+} ions. The fact that cooperative luminescence line-shape is proportional to the self-convolution integral of that of the NIR emission spectrum confirms its origin in the presence of Yb^{3+} IP [29].

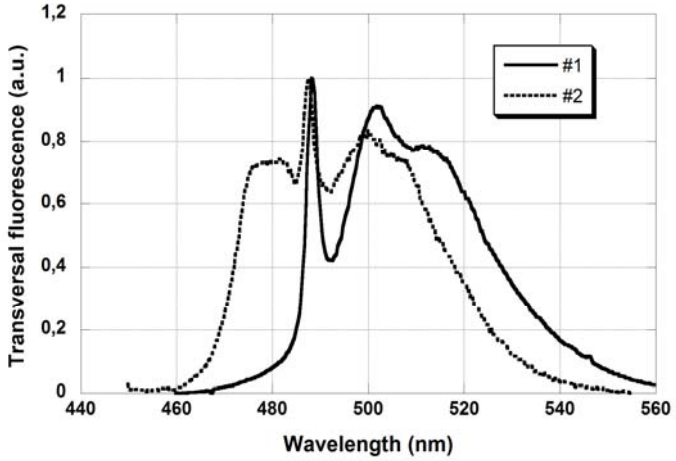

Fig. 1: Emission spectra of the DC Yb-doped fibres #1 and #2 in the visible range

The decay times of the visible cooperative emission at $\lambda \approx 0.5$ μm have been measured after pump switch off using a digital storage oscilloscope. The experimental power decays are shown in Fig. 2 together with fits by a single exponential. Lifetimes values are 0.40 ms (F#1) and 0.65 ms (F#2). As could be expected for each fibre cooperative lifetimes are about half of the NIR values. Lifetime increase with the absorption coefficient (and subsequently with Yb^{3+}-ion concentration) seems to indicate that radiation trapping predominates over migration-induced non-radiative loss processes [30]. From Fig. 2 it is clear that decay curves exhibit a single exponential nature for both concentrations. In Ref. [14] they claimed that two exponentials were

needed for a satisfactory fit of the NIR luminescence power decays and the second exponential is attributed to the process of excitation relaxation in Yb^{3+} IPs.

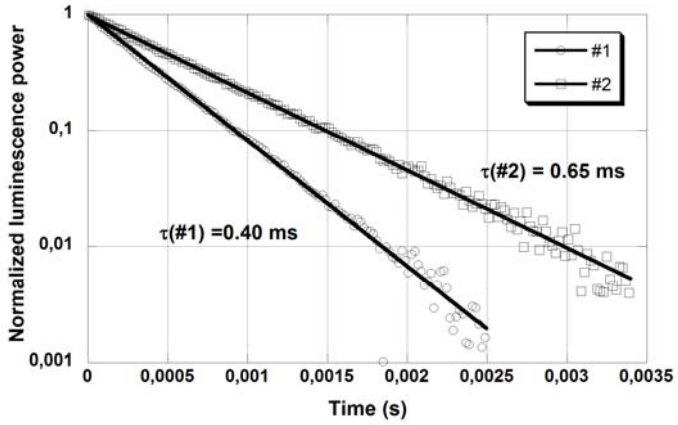

Fig. 2. Experimental visible luminescence power decays in fibres #1 and #2 after pump switch-off and single-exponent fits.

3.2. The double clad Yb-doped fibre laser.

A laser setup in a ring configuration was built using two optical combiners at both ends of the DC Yb-doped fiber, an isolator to favour counterpropagating ASE and a directional coupler to extract the laser power from the cavity.

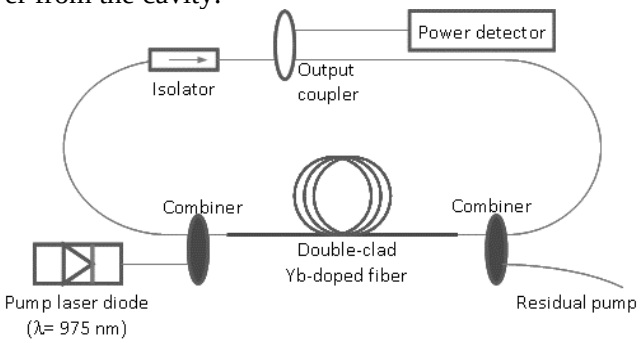

Fig. 3. Laser ring configuration setup.

Pump power from a ≈975-nm laser diode was launched into the DC Yb-doped fiber. The maximum pump power at the fiber input end was 5.87 W and the pump power spectrum depended on the total pump power as it is shown in Fig 3. in Ref. [13]. The parameters of the laser performance (pump power threshold, efficiency and maximum output power) for fibres #1 and #2 and for different fibre lengths and ring cavity input/output coupling rates are also summarized in Ref.[13]. Laser peak emission wavelength was between 1090 nm and 1100 nm. The transmission and isolation spectral dependences of the ring scheme components (an Isolator IO-F-1064APC and the couplers FFS-064C52A10 (20/80) and FFS-064E52A10 (30/70) from Gooch & Housego) guarantee that their changes in a few-nm laser emission bandwidth have a negligible influence on the laser output power. This assumption is validated by the good fits obtained in Ref.[13], and there is no special reason for a more critical spectral dependence of the ion-pairs effect.

4. Evaluation of the ion-pairs influence on the laser performance

Although the cooperative luminescence intensity spectra are many orders of magnitude weaker than IR emission [8], influence of ion pairs induced processes has been claimed to be decisive to describe pump propagation along the highly-doped fibre [14]. In order to assess the effective influence of IPs through CL in the laser performance we use the model described in section 2.3 and validated in Ref. [13] to calculate the laser output powers assuming different values of C_p

for both fibres. The excellent agreement between experimental and numerical results neglecting IPs contribution in Ref. [13] already pointed to its small influence. In Fig. 4 laser output powers are plotted for different values of C_p for F#1 and F#2 as a function of the laser input pump power. For each fibre the minimum value of C_p required for a significant effect of IPs in the laser output power can be estimated from Fig. 4 by comparing the plotted results with those for $C_p \neq 0$. As could be expected, due to the significantly higher concentration in fibre #2, a similar cooperative coefficient causes a larger variation in the laser output powers.

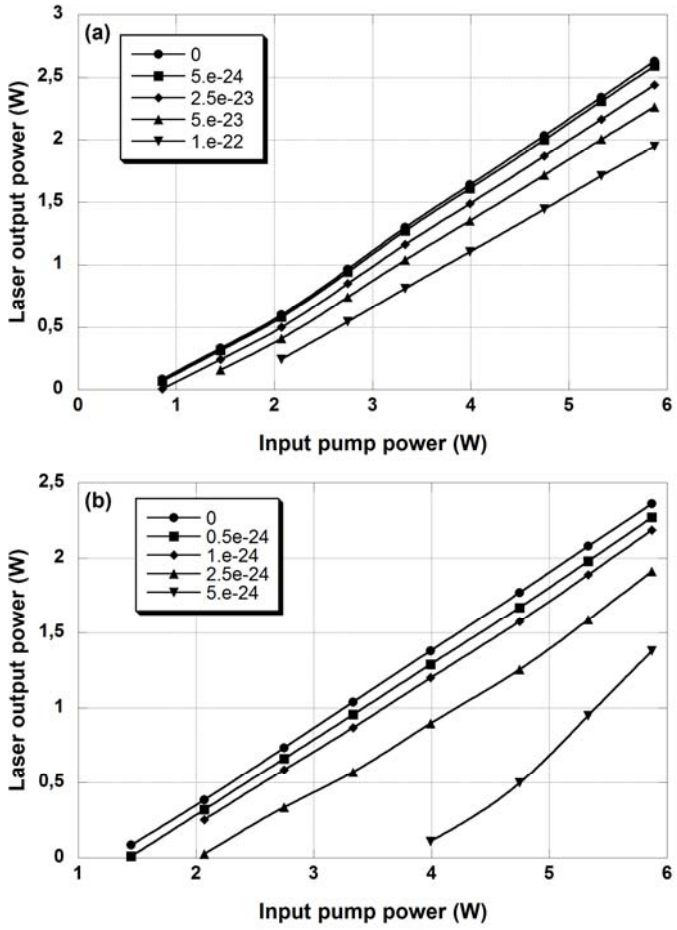

Figure 4. Laser output powers are plotted for different values of C_p for (a) F#1 and (b) F#2

Assuming a theoretical value for Yb interaction distances in the range 3-5 Å (including exchange, electrostatic and magnetic interactions) [31] we obtain $C_p = 4.3x10^{-29} s^{-1}m^3$. In what regards experimental values comparable C_p coefficients can be found for different hosts: 2.8 x 10^{-28} $s^{-1}m^3$ [32] and 2.6 x 10^{-28} $s^{-1}m^3$ [33]. As can been seen from Fig. 4, with these values for the C_p coefficient the effect of the IPs–related mechanisms in the laser performance is totally negligible.

In Ref. [14] they assess the effect of IPs using the parameter, τ_p, the so called pairs' relaxation parameter in a n_{Yb} – normalized excited state population rate equation. The two parameters C_p and τ_p can be straightforwardly related according to $C_p = \left(2\tau_p n_{Yb}\right)^{-1}$. They report a value of $\tau_p = 0.1\,ms$ for a fibre (#5 in Ref. [14]) with a similar concentration to F#1. From Fig. 4(a) it is seen that with the high corresponding cooperative coefficient $C_p = 1.4x10^{-23} s^{-1}m^3$ the laser

output power would slightly decrease. It has to be remarked that the maximum pump power in Ref. [14] was 200 mW (more than one order of magnitude lower than in our experiments) and therefore the fraction of excited single atoms for a similar concentration had to be much lower and subsequently the intensity of visible cooperative luminescence, what reinforces the conclusion that the role of IPs was overestimated. Logically, as it is plotted in Fig.4(b), for a higher concentration (12×10^{26} m^{-3}) this effect becomes significant for a lower ion-pairs coefficient but still 3 orders of magnitude higher than the other coefficients in the literature.

5. Conclusions

The real effect of Yb^{3+}-ion pairs induced cooperative processes in the performance of highly Yb-doped amplifiers and lasers is an still unclear issue. We have made numerical simulations of the output power of a ring configuration double-clad Yb-doped fibre laser and when theoretical or experimental values are considered for cooperative coefficients IPs contribution to the laser performance is totally negligible. Our simulations reinforce the statement that effective influence of IPs in the laser output power has sometimes been overestimated.

Acknowledgements
This work has supported by the Spanish Ministry of Economy and Competitiveness under the TEC2013-46643-C2-2-R project, by the Diputación General de Aragón and by the Fondo Social Europeo.

References:

[1] Limpert J, Röser F, Klingebiel S, Schreiber T, Wirth C, Peschel T, Eberhardt R and Tünnermann A 2007 *IEEE J. Sel. Topics. Quantum Electron.* **13** 537-45
[2] Zervas M. N. and Codemard C. A. 2014 *IEEE J. Sel. Topics. Quantum Electron.* **20** 219-241
[3] Gu G, Liu Z, Kong F, Tam H, Shori R K and Dong L 2015 *Optics express* **23** 17693-17700
[4] Glick Y, Fromzel V, Zhang J, Dahan A, Ter-Gabrielyan N, Pattnaik R K and Dubinskii M 2016 *Laser Physics Letters* **13** 065101
[5] Guiraud G, Traynor N and Santarelli G 2016 *Optics Letters* **41**4040-4043
[6] Hou C, Zhu Y, Zheng J, Li G, Li C, Gao S, Gao Q, Zhang L, Chang C, Zhao W, Li W and Zhao B 2016 *Optical Materials Express* **6** 979-985
[7] Paschotta R, Nilsson J, Barber P R, Caplen J E, Tropper A C and Hanna D C 1997 *Opt. Commun.* **136** 375-8
[8] Bell M J V, Quirino W G, Oliveira S L, de Sousa D F and Nunes L A O 2003 *Journal of Physics: Condensed Matter* **15** 4877-87
[9] Auzel F., Baldacchini G., Laversenne L. and Boulon G. 2003 Opt. Mat. **24** 103-109
[10] Nakazawa E and Shinoya S 1970 *Phys. Rev. Lett.* **25** 1710-2
[11] Choi Y G, Shin Y B, Seo H S and Kim K H 2002 *Chemical physics letters* **364** 200-205
[12] Rybaltovsky A A, Aleshkina S S, Likhachev M E E, Bubnov M M, Umnikov A A, Yashkov M V, Gur'yanov A N and Dianov E M 2011 *Quantum Electronics* **41** 1073-1079
[13] Vallés J A, Berdejo V, Martin J C,Cases R, Álvarez J M and Rebolledo M A 2016 *Laser Phys.* **26** 125105
[14] Kiryanov A V, Barmenkov Y O, Martínez I L, Kurkov A S and Dianov E M 2006 *Opt. Express* **14** 3981-92
[15] Boulon G 2008 *J. Alloys Compd*. **451** 1-11
[16] Schaudel B, Goldner P, Prassas M and Auzel F 2000 *Journal of alloys and compounds* **300** 443-449
[17] Babu P, Martín I R, Venkataiah G, Venkatramu V, Lavín V and Jayasankar C K 2016 *Journal of Luminescence* **169** 233-237
[18] Montoya E, Espeso O and Bausa L E 2000 *Journal of luminescence **87*** 1036-1038
[19] Diaz-Torres L A, De la Rosa E, Salas P and Desirena H 2005 *Optical Materials **27*** 1305-1310
[20] Puchalska M, Sobczyk M, Targowska J, Watras A and Zych E 2013 *Journal of Luminescence* **143** 503-509
[21] Guan Y, Huang Y and Seo H J 2012 *Materials Letters* **89** 126-128
[22] Malinowski M, Kaczkan M, Piramidowicz R, Frukacz Z and Sarnecki J 2001 *Journal of luminescence* **94** 29-33
[23] Ryan T G and Jackson S D 2007 *Optics communications* **273** 159-161

[24] Vázquez G V, Desirena H, De la Rosa E, Flores-Romero E, Márquez H, Rickards J and Trejo-Luna R 2012 *Optics Communications* **285** 5531-5534
[25] Koponen J, Söderlund M, Hoffman H J, Kliner D A, Koplow J P and Hotoleanu M 2008 *Applied optics* **47** 1247-1256
[26] Imanieh M H, Martín I R, Eftekhari Yekta B, Marghussian V K and Shakhesi S 2012 *Journal of the American Ceramic Society* **95** 3827-3833
[27] Qin W P, Liu Z Y, Sin C N, Wu C F, Qin G S, Chen Z and Zheng K Z 2014 *Light: Science & Applications* **3** e193
[28] Gebavi H, Taccheo S, Milanese D, Monteville A, Le Goffic O, Landais D, Mechin D, Tregoat D, Cadier B and Robin T 2011 *Opt. Express*, **19** 25077-25083
[29] Magne S, Ouerdane Y, Druetta M, Goure J P, Ferdinand P and Monnom G 1994 *Optics communications* **111** 310-316
[30] Yoshikawa A, Boulon G, Laversenne L, Lebbou K, Collombet A, Guyot Y and Fukuda T 2003 *J. Appl. Phys.: Condens. Matter* **94** 5479–5488
[31] Goldner Ph, Pelle F and Auzel F 1997 *J. Lumin.* **72-74** 901-903
[32] Goldner Ph, Pelle F, Meichenin D and Auzel F 1997 *J. Lumin.* **71** 137-150
[33] Courrol LC, Samad RE and Madej C 2000 *Ann. Braz. Comission Opt.* **2** 102-104